2024 IEEE International Conference on Robotics and Automation (ICRA 2024)
May 13-17, 2024. Yokohama, Japan

Odometry Estimation by Fusing Multiple Radar Sensors and an Inertial Measurement Unit

Tim Brühl[1,2], Tim Dieter Eberhardt[1,3], Robin Schwager[1,2],
Lukas Ewecker[1], Tin Stribor Sohn[1] and Sören Hohmann[2]

***Abstract*— This paper presents a framework for odometry estimation in automotive application using six asynchronously operating millimeter wave radar sensors and a combination of gyroscope and accelerometer. Two different motion models are combined to estimate motion with three degrees of freedom. For this purpose, we propose a novel three-part radar filtering method for outlier detection: By analyzing uncertainties and system limits, sensor-specific outliers are detected and removed in the first filter. We introduce knowledge about the previous motion state by a status-quo-ante filter and hereby identify further false positive raw targets in the current measure which are not accessible from the previous state. Moreover, we suggest employing a downstream, resampling-based algorithm for additional outlier detection. Based on the filtered data, radar motion state estimation is performed by use of curve fitting methods. To fuse the radar odometry estimation with the acceleration and yaw rate measurements handling non-linearities, an Unscented Kalman Filter is used. The developed framework is evaluated with reference data in various scenarios. The results demonstrate that it accurately and robustly determines motion and position states even in radar-challenging scenes, such as environments with few radar targets or with heavy metal structures. Our method keeps up with common approaches such as wheel speed sensor odometry while outperforming it in terms of drift-impairment.**

I. INTRODUCTION

Automated driving makes traffic more convenient and safe. Robotic systems can relieve the driver of such tedious tasks. E. g. parking functions are able to maneuver the vehicle for the last meters in parking planes or garages. This can safe time for the driver and clears them of the charge to drive in a cramped, dark environment with many obstacles which are rarely visible. Based on an environmental model, a trajectory is planned and the actors are controlled to guide the vehicle on this trajectory. One way to represent trajectories is by a number of consecutive states featuring position, yaw angle, wheel angle, speed and yaw rate attributes each [1]. For the purpose of controlling the trajectory with minor control error, it is essential that the vehicle has precise knowledge about its state of movement.

Moreover, for tasks like localization, based on a current pose a rough guess for the consecutive pose is performed by transforming the vehicle along its current motion. At this, the velocity and yaw rate signals are integrated over time to calculate the pose shift between two steps [2].

In the past, a common way to determine the movement of the vehicle has been by incrementing wheel speed signals. By knowing its wheel base, the velocity of the vehicle and its current curve radius can be calculated. However, this approach leads to drifts during the integration of yaw rates and velocities to yaw angles and positions [3]. Second, in the case that wheelspin occurs, the odometry estimation will give wrong values. To avoid those drawbacks, using the perception sensors of the vehicle might be a beneficial approach.

A modern vehicle is equipped with multiple environmental perception sensors. The purpose of the radar sensors is mainly to detect moving objects. It has major strengths in the determination of distances and velocities. However, the occurrence of radar raw targets is rather sparse [4]. In the automotive case of application, the camera is typically used for traffic sign detection and recognition as well as lane marking detection [5]. Except these sensors, modern vehicles are equipped with an Inertial Measurement Unit (IMU) which measures rotational speeds and accelerations. Its primary objective is the determination of parameters for vehicle dynamic systems such as the electronic stability control or the airbag system release times for vehicle safety. In this paper, a novel approach for the fusion of radar and IMU sensors to determine the vehicle odometry is investigated. Visual Odometry based on the cameras is not investigated since we look for a robust approach which also works in poorly illuminated areas and with soiled camera lenses.

The fundamental challenge when using radar sensor generated data is the detection of outliers. Due to the noise of radar data, targets like clutter and false positives need to be extracted. For this reason, we introduce the status-quo-ante filter approach which removes impossible targets from the input set. Besides, we show how to fuse the radar odometry estimation with the IMU sensor to receive a more robust motion estimate in a three Degrees of Freedom (DoF) model. The use of this model proved beneficial due to lateral shifts which can occur especially in parking environments when curbs are overrun. Due to the non-linearity of the motion mode, we use an Unscented Kalman Filter (UKF) for the fusion of the radar and the IMU.

Note that, while most of the elements in our pipeline, such as M-Estimator Sample Consensus (MSAC), Least Squares Estimation (LSE), and UKF, are widely investigated already,

(Tim Brühl and Tim Dieter Eberhardt are co-first authors.)
[1]Dept. of Highly Automated Driving Systems, Dr. Ing. h.c. F. Porsche AG, Weissach, Germany {tim.bruehl, robin.schwager1, lukas.ewecker, tin_stribor.sohn}@porsche.de
[2]Institute of Control Systems, Karlsruhe Institute of Technology, Germany soeren.hohmann@kit.edu
[3]Hochschule für Technik und Wirtschaft, Berlin, Germany tim.eberhardt@student.htw-berlin.de

in this work, these tools are assembled to a new pipeline. It takes advantage of the excellent velocity measuring capability of radar sensors. Creating redundancy is a demand to ensure safety in systems with a high level of automation and can be achieved by fusion with a second sensor type. The error-proneness can be lowered by using a radar setup with sensors directed to different directions. The system is able to deal with asynchronous data.

The developed method is evaluated during a real-world test drive. Following questions which occurred from the problem shall be answered:

1) Does a fusion of radar odometry and IMU improve the path accuracy?
2) How does the system react to sudden changes in the motion dynamic?
3) Is the system suitable to estimate driven paths free of drift effects?

The structure of our work is outlined as follows. We analyze the State-of-the-Art of radar odometry, explain the principle of motion estimation based on radar targets and elaborate our single approaches in the modules filtering, outlier detection, estimation and Kalman filtering. We conducted an experiment with a test vehicle in an outdoor parking area. The data from an additionally installed Real Time Kinematic (RTK) as well as from the established method involving the wheel speed sensors serve as basis for comparison with our approach. The results are discussed, before we summarize our work and go into detail about plans for future investigations.

II. RELATED WORK

There is comprehensive research about using environmental perception sensors for odometry estimation. Early approaches on employing camera-captured images for motion estimation try to recognize patterns in two consecutive images. Nistér et al. employ corners found by the Harris corner detector in an image recorded by a monocular camera as features [6]. The motion is then estimated with a Random Sample Consensus (RANSAC) model [7], which samples multiple feature correspondences and takes the best-matching hypothesis. Meanwhile, most of the research focuses on semi-direct or direct visual odometry, as He et al. state [8]. These methods minimize the reprojection error of points from the three-dimensional world back to the two-dimensional camera image, the so-called photometric error.

Heading towards direct registration methods can also be noticed for lidar odometry. In the past, various works were based on features which are first extracted and then matched between two point clouds. The idea is to minimize a distance metric between two point clouds by transforming one to the other. Segal et al. [9] proposed the Generalized-Iterative Closest Point (ICP) which combines standard ICP with an algorithm that minimizes the error from the point to the surface normal in place of another point, called point-to-plane.

Fresher works concentrate on direct registration since higher performance can be achieved. Zhang and Singh concentrated on direct registration to achieve higher performance. They split the problem in two functions, one doing a rough estimation of the odometry very often and a second one which registers the point cloud very exact, but at a lower frequency [10]. Xu et al. achieve fast LiDAR-based odometry by building a map of registered points, which is represented by an incremental tree data structure [11].

The idea of key point extraction and matching was transferred to radar [12], partially also to apply it for Simulataneous Localization and Mapping (SLAM) [13]. However, point set registration can be complex for radar sensors, as radar point clouds are noisy and generally sparse. Conversely, radar raw targets deliver the relative velocity as a directly measured attribute with them. This made Kellner et al. [14] propose an approach to determine the vehicle odometry of radar sensors in one single shot. Further work of them extended the work to two sensors [15]. This allows for estimation of a yaw rate ω in addition to the longitudinal velocity v_x. Modern vehicles are usually equipped with more sensors than just perception sensors. Still, the problem arises how to combine these sensors for estimating motion as accurate as possible. Doer et al. [16] showed how 3-DoF odometry estimation can be improved by making use of an IMU as a second element, combining both by filtering the observations and states in an Extended Kalman Filter (EKF). They presented experiments with a drone, measuring its odometry in a Global Navigation Satellite System (GNSS)-denied area. Further work of them proposed Manhattan world assumptions for a yaw aided odometry estimation. Their algorithm additionally searches the environment for planar surfaces and tracks the change of their yaw angle, choosing the most likely yaw rate by Bayesian interference [17].

Ghabcheloo and Siddiqui combine a single automotive radar sensor with a gyroscope to estimate velocity and yaw rate of a small wheel loader. After classifying stationary radar raw points, a motion vector is determined from a point tuple. The resulting motion vectors from multiple point tuples are averaged - a method which is prone to outliers and aberrant values [18]. Next, outliers were detected via RANSAC. However, the motion estimate results from a combination of v_x and v_y determined by radar odometry as well as ω measured by the gyroscope. Hence, no fusion of independently measured values has been undertaken. Furthermore, it is not outlined how noise points were removed [19]. Similar proceeding is described in [20]: A pipeline is employed with RANSAC for outlier detection and a Constant Turn Rate and Velocity (CTRV) motion model in which the yaw rate measured by an IMU completes the radar linear velocity estimates. Only radar ground reflections were used. Kramer et al. show an application to estimate the velocity vector $[v_x, v_y, v_z]^\mathsf{T}$ of 4D radars and use IMU data to bridge longer radar measurement intervals [21].

Comprising the related work, we found that radar-based odometry estimation for automotive application, using multiple radar sensors in a belt, and applying further sensors which are commonly installed in road vehicles, has not been

investigated before. This induced us to implement our own pipeline, which is explained in the following section.

III. Radar Odometry Estimation

In this section, we present an approach for 3-DoF vehicle motion estimation by using raw targets of radar sensors which are arranged in a belt-like manner around the vehicle.

We introduce the concept of single-shot radar odometry estimation. Next, we describe the single components of the algorithm: raw target constant filtering, status-quo-ante filtering, resampling-based MSAC filtering, and the two-part parameter estimation. The achieved radar odometry can be used for a fusion with an IMU sensor output in a next step.

A. Motion Determination by Radar Sensors

The motion determination algorithm is related to Kellner's approach in [15]. It can be applied for a set of j radar sensors $\boldsymbol{S} = S_1, \ldots, S_j$. In a first step, each sensor's velocity is estimated based on the distribution of the radial velocities v_D over the azimuth angle θ. Such a radial velocity $v_{D,n}$ can directly be measured for each of the $n = 1, \ldots, N$ raw targets received by the respective sensor. First, the velocity $\boldsymbol{v_S}$ of one radar sensor S in x- and y-direction is determined by solving

$$\underbrace{\begin{bmatrix} -v_{D,1} \\ \vdots \\ -v_{D,N} \end{bmatrix}}_{\boldsymbol{v_D}} = \underbrace{\begin{bmatrix} \cos(\theta_1) & \sin(\theta_1) \\ \vdots & \vdots \\ \cos(\theta_N) & \sin(\theta_N) \end{bmatrix}}_{\boldsymbol{M}} \underbrace{\begin{bmatrix} v_{x,S} \\ v_{y,S} \end{bmatrix}}_{\boldsymbol{v_S}}. \tag{1}$$

The motion state vector $\boldsymbol{m} = [\omega, v_x, v_y]^\mathsf{T}$ of the vehicle is given by the positions of the detecting radar sensors $x_{c,S1}, y_{c,S1}, \ldots, x_{c,Sj}, y_{c,Sj}$ with respect to their velocity vectors $\boldsymbol{v_{S_1}}, \ldots, \boldsymbol{v_{S_j}}$.

$$\underbrace{\begin{bmatrix} v_{x,S_1} \\ v_{y,S_1} \\ \vdots \\ v_{x,S_j} \\ v_{y,S_j} \end{bmatrix}}_{[\boldsymbol{v_{S1}}, \ldots, \boldsymbol{v_{Sj}}]^\mathsf{T}} = \underbrace{\begin{bmatrix} -y_{c,S1} & 1 & 0 \\ x_{c,S1} & 0 & 1 \\ \vdots & \vdots & \vdots \\ -y_{c,Sj} & 1 & 0 \\ x_{c,Sj} & 0 & 1 \end{bmatrix}}_{[\boldsymbol{S_1}, \ldots, \boldsymbol{S_j}]^\mathsf{T}} \underbrace{\begin{bmatrix} \omega \\ v_x \\ v_y \end{bmatrix}}_{\boldsymbol{m}}. \tag{2}$$

In eq. 2, it must hold that at least two sensors with different position parameters are applied ($j \geq 2$) to determine the motion state vector $\boldsymbol{m}$. If sensors are mounted symmetrically, their matching is prohibited due to the similar lever length. Consequently, there are only three pairs of prohibited sensor combinations: (FL, FR), (ML, MR) and (BL, BR).

Preventing the case to use a prohibited combination of sensors for the motion determination is essential and controlled in our approach. Combining Eq. 1 and 2 results in the complete system motion equation

$$\begin{bmatrix} v_{D,S_{1,1}} \\ \vdots \\ v_{D,S_{j,N}} \end{bmatrix} = \begin{bmatrix} \boldsymbol{M_1 S_1} \\ \vdots \\ \boldsymbol{M_j S_j} \end{bmatrix} \begin{bmatrix} \omega \\ v_x \\ v_y \end{bmatrix}. \tag{3}$$

Taking the k[th] row of the equation 3, the velocity profile yields

$$-v_{D,k} = \Big(-y_C \cos(\theta_k) + x_C \sin(\theta_k)\Big)\omega + v_x \cos(\theta_k) + v_y \sin(\theta_k). \tag{4}$$

B. Constant Filtering

We removed outliers from the data which was captured from the sensors by applying static filtering. A typical effect is that the interference of radar waves causes ghost detections. However, they can be filtered by their characteristic velocity. Body parts of the vehicle, which are parallel to the radar antennas, lead to reflections close to the sensors, which exhibit an azimuthal angle of $0°$. False Positive detections can be caused by effects such as e.g. interference [22], but they often show a low signal power. For this reason, we filter all signals with a signal power below SNR $= 50\,\mathrm{dB}$, with a distance of more than $90\,\mathrm{m}$ and with an angle of exactly $0°$.

C. Status-Quo-Ante Filtering

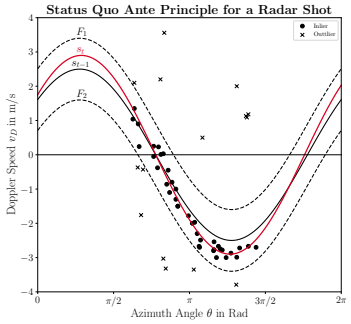

Fig. 1: Schematic visualization of the Status Quo Ante Principle for outlier classification

The main idea is to apply knowledge about the previous system states x_{t-1} and the system behavior to the outlier detection problem of the current state x_t (s. figure 1). The system changes its motion state between two measurements, which have a time delta of only $0.02\,\mathrm{s} \leq \Delta t \leq 0.06\,\mathrm{s}$, only to a limited multitude.

As our goal is to apply the algorithm for motion estimation in an automotive use case, we assume a maximum deceleration of $a_{x,min} = -15\,\frac{\mathrm{m}}{\mathrm{s}^2}$ (emergency braking) and a maximum acceleration of $a_{x,max} = 11\,\frac{\mathrm{m}}{\mathrm{s}^2}$. These assumptions define the system boundaries. Using these boundaries, we form a channel defined by the filter function $\mathcal{F}$ around the velocity profile 4. This filter incorporates only motion changes which are physically possible. Any non-plausible states that are outside of this channel are discarded.

$$\mathcal{F}_{1,2}(\theta) = -v_D(\theta, \omega_{t-1}, v_{x,t-1}, v_{y,t-1}, x_{c,t-1}, y_{c,t-1}) \pm T_F \tag{5}$$

T_F is the threshold value which is to be determined according to the expected vehicle dynamics. Using the case of an emergency braking, the threshold is determined by the maximum change $\triangle v_x$ of the longitudinal velocity

$$T_F = \triangle v_x = a \cdot t \approx 15\,\frac{\mathrm{m}}{\mathrm{s}^2} \cdot 0.06\,\mathrm{s} = 0.9\,\frac{\mathrm{m}}{\mathrm{s}}. \tag{6}$$

D. MSAC Algorithm

In this work, we present radar outlier detection by applying the MSAC algorithm [23]. Earlier work used RANSAC [7] as an outlier detection, which randomly samples sets of measures, determines the model parameters for this set and calculates the consensus set of remaining measures which support the current model. Hence, the consensus set is improved iteratively, saving the model parameters if the consensus set outperformed all previous ones. However, since RANSAC weights outliers constantly, the severity of the outlier does not have an impact on the decision if it belongs to a fitting set. MSAC addresses this deficiency by weighting each measure according to its error. It minimizes the cost function

$$C = \sum_i \rho(e_i^2) \tag{7}$$

with ρ as

$$\rho(e_i^2) = \begin{cases} e^2 & e^2 < T^2 \\ T^2 & e^2 \geq T^2. \end{cases} \tag{8}$$

By defining a threshold T, the mentioned weighting for each error of a point e is realized. Applying the previous constant filter and status-quo-ante filter with 5, a prior choice of the data to find the best model the MSAC algorithm is used. Like the RANSAC algorithm, the MSAC algorithm needs several iterations n_{Iter}. As proposed by [7], we calculated 17 iterations, improving the consensus set in each.

E. Parameter Estimation

For the parameter estimation, we use a conventional LSE method. The parameters $\hat{\beta}$ are estimated with the formula

$$\hat{\boldsymbol{\beta}} = (\boldsymbol{X}^{\mathsf{T}}\boldsymbol{X})^{-1}\boldsymbol{X}^{\mathsf{T}}\boldsymbol{y}. \tag{9}$$

The independent variable $\boldsymbol{X}$ is the azimuthal position of a radar target θ, while the dependent variable $\boldsymbol{y} = f(X, \hat{\beta}) - \epsilon(y)$ is the measured relative Doppler velocity v_D of this target. The LSE method is problematic for our use case since it incorporates only errors in the dependent variable $\boldsymbol{y}$, meaning that the relative Doppler velocity v_D is assumed to be erroneous with an additional error $\epsilon(y)$, whereas the measured azimuth angle θ is considered as faultless. This does not reflect the properties of radar raw measurements, where the azimuth angle error $\epsilon(X)$ can be considered as more significant than the Doppler velocity error. For this reason and just as proposed by Kellner et al. [14], we implemented a downstream Orthogonal Distance Regression (ODR) algorithm. This algorithm solves the optimization problem

$$\min_{\hat{\beta}, \epsilon(X)} \sum_{i=0}^{n} \left\{ [f(X_i + \epsilon(X_i), \hat{\beta}) - y_i]^2 + \epsilon(X_i)^2 \right\} \tag{10}$$

which is initialized by the solution of the LSE (ODR $\leftarrow$ LSE). Further tests while the vehicle was at rest showed that in approximately empty environments the ODR regression method determines implausible results (Standard deviation of the v_x-estimations: $\sigma_{\text{LSE}} = 0.0004\,\frac{\text{m}}{\text{s}}$, $\sigma_{\text{ODR}} = 30.05\,\frac{\text{m}}{\text{s}}$). For this purpose, an extra control function is implemented which controls the estimator. If the number of targets n_{CF} after the constant filter is less than the minimum needed number for the MSAC algorithm, only LSE is used. Otherwise, estimation of the parameters happens during a combination of ODR and LSE.

$$\hat{\boldsymbol{\beta}} = \begin{cases} \text{LSE} & n_{CF} < n_{\text{Iter}} \cdot 2 \\ \text{ODR} \leftarrow \text{LSE} & n_{CF} \geq n_{\text{Iter}} \cdot 2. \end{cases} \tag{11}$$

Given the asynchronous operation of two radar sensors, the shots are only received successively for estimation. Thus, during combination in Eq. 3, errors may occur due to this time difference. To prevent this, the possible error has to be limited. We consider that the maximum error owing to the time delay has to be equal to the maximum error regarding the measurement uncertainties in Table I. As a result, we determine a maximum time difference of $t_{S,max} = 0.03\,\text{s}$. Compounding this limitation and the prohibited cases, a multiplexer combines these functions and controls the input of the filter and the following estimator.

IV. FUSION OF RADAR AND IMU DATA

The radar odometry estimation approach described in section III can be used on its own. However, an IMU consisting of at least an accelerometer and a gyroscope is available in most modern vehicles. We hold the opinion that available sensors should be used to further improve the precision and robustness of the estimate. In this section, we introduce the two used motion models which showed requisite and their combination for our purpose. Besides, we state how a state filter such as an UKF can be applied for multi sensor fusion.

A. Motion model

We receive data from both the radar sensors and the IMU sensor discretely with a cycle time of 0.06 s (radar sensors) and 0.01 s (IMU). Between two measurement time stamps t_0 and t_1, the respective motion state is assumed to be constant. Firstly, the radar sensor-based method directly outputs the velocities v_x, v_y, and the yaw rate ω. Secondly, the IMU sensor measures the longitudinal acceleration a_x and the yaw rate ω. To combine radar and IMU measurements, we define the following assumptions:

- Constant longitudinal acceleration, $a_x = \text{const.}$
- Constant yaw rate, $\omega = \text{const.}$
- No consideration of lateral acceleration, $a_y = 0\,\frac{\text{m}}{\text{s}^2}$.

The assumptions are a result of typical IMU sensor properties, which can measure longitudinal as well as lateral acceleration and three-axis turn rates, but do not provide data about the yerk $\frac{da}{dt}$ or the yaw acceleration $\frac{d\omega}{dt}$. Since parking maneuvers are investigated in particular, the assumptions form a valid base for the subsequent considerations.

We point out that the IMU-measured y-directed acceleration a_y equals the centripetal acceleration of the car and cannot directly be used to model the vehicle motion. The motion is hereby described as a vector $m = [v_x, v_y, \omega]^{\mathsf{T}}$,

while the position is held by the vector $\boldsymbol{p} = [x_{KK}, y_{KK}, \psi]^\mathsf{T}$. With consideration of the longitudinal acceleration $a = a_x$ the whole state of the vehicle at the time t is described by the vector:

$$\boldsymbol{s(t)} = [x_{KK}, y_{KK}, \psi, v_x, v_y, \omega, a]^\mathsf{T}. \tag{12}$$

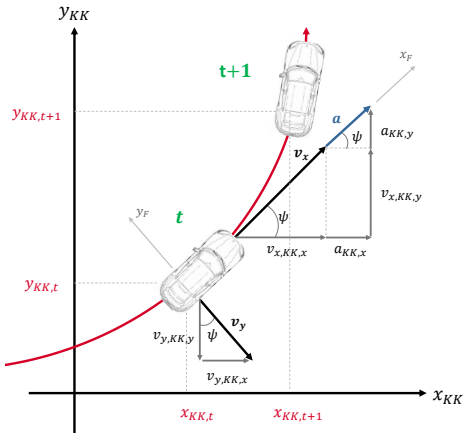

Fig. 2: Schematic representation of the vehicle movement during cornering

In figure 2, the components that contribute to the change in the position of the vehicle are represented as vectors. The reference point of the vehicle is arbitrary and set to the middle of the rear axis.

The desired resulting position of the vehicle $x_{KK,t+1}, y_{KK,t+1}$ in the map coordinate system *KK* is determined by integration over all the components which contribute to the movement in the direction of x_{KK} and y_{KK}, respectively.

The position can be determined either by the linear (L) or curvilinear (CL) motion model by integration, choosing CL only if a yaw rate $\dot{\psi} \geq 0.04\,\frac{\mathrm{m}}{\mathrm{s}^2}$ is determined, since numerical instabilities may occur for small yaw rates $|\dot{\psi}| < 0.04\,\frac{\mathrm{m}}{\mathrm{s}^2}$.

The angle of the vehicle ψ and velocity in x-direction v_x is received by integration of ω and a over time.

B. UKF Multi Sensor Fusion

An established way to fuse two different sensors is to use Kalman filters. The idea behind Kalman filters is the continuous estimation of a state and its uncertainty using a state model and an observer model. As our field of application is non-linear, it demands approaches that can cope with this circumstance. Doer et al. [16] showed for our field of application that sensor fusion can be performed by using an EKF. However, the EKF may lead to a non-converging filter and be inaccurate [24]. For this reason, we investigated fusion by an UKF [25]. This approach propagates sigma points which hold the mean and covariance of a Gaussian random variable. To create these sigma points, the Van der Merwe's algorithm [26] is used. As the parameter set, we chose $\alpha_\chi = 0.5$, $\beta_\chi = 0.5$ and $\kappa_\chi = 10000$ [27].

The final output of the UKF is the state vector $\boldsymbol{s(t)}$. Figure 3 provides an overview of our entire, proposed framework.

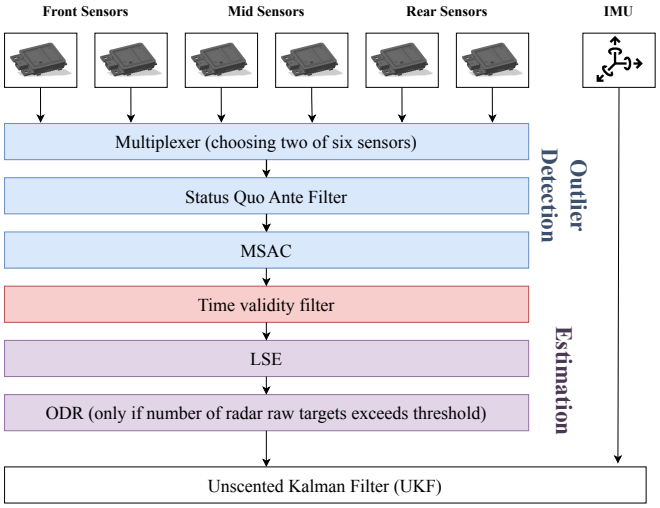

Fig. 3: Pipeline which contains the steps outlier detection, parameter estimation and sensor fusion

V. EXPERIMENTS

We conducted an experiment to determine the performance of the proposed algorithm estimating the ego motion of our test vehicle.

A. Vehicle setup

TABLE I: Radar sensor properties

Band Width	600 MHz
Distance Field-of-View (FoV)	92.0 m
Azimuth angle FoV	±75°
Angle accuracy	0.15 °
Velocity accuracy	0.02 $\frac{\mathrm{m}}{\mathrm{s}}$
Update rate	0.06 s

As a carrier for the radar sensors, we use a Porsche Cayenne Mk3. The radar sensors are commercially available and mounted behind the front and rear bumper and in the side panel on the same level with the b-pillar. The technical characteristics of the radars and its FoV are listed in the table I.

B. Outdoor environment

The drive features a part with less targets as well as a part with higher velocities and a reverse parking process. We decided for an outdoor test due to availability of high precision RTK data. The overall distance of the trajectory is $d = 315.9\,\mathrm{m}$ driven in a time of $t = 106.6\,\mathrm{s}$ with the velocity being in the dimension of walking pace for most of the time, but up to $24.3\,\frac{\mathrm{km}}{\mathrm{h}}$. Additionally to the wheel speed sensors, the outdoor environment facilitated the use of an RTK system to record a ground truth for the motion estimation. Figure 4 shows the velocity profiles of both motion estimates. The root-mean-square error (RMSE) metrics are listed in table II.

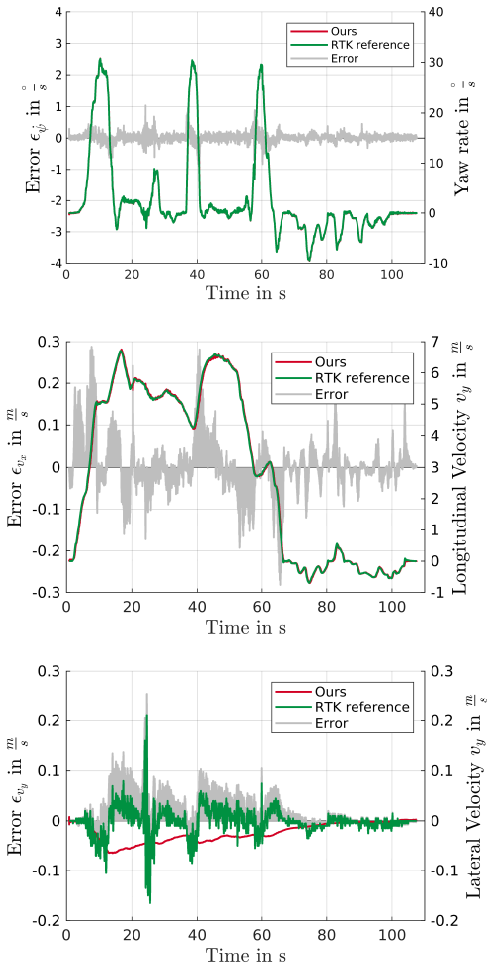

Fig. 4: Velocity profile

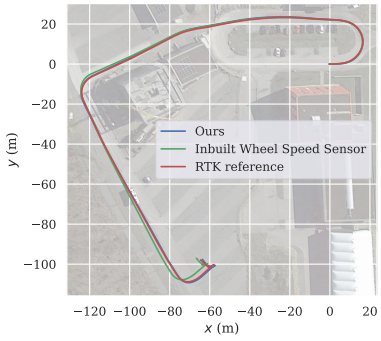

Fig. 5: Determined trajectory by our approach, a reference and the wheel speed sensor are plotted for comparison

TABLE II: Errors of our odometry estimation, referenced to the RTK system

Error	v_x	v_y	$\dot{\psi}$
ϵ_{RMSE}	0.0589 $\frac{m}{s}$	0.0422 $\frac{m}{s}$	0.0808 $\frac{°}{s}$

Besides, we compare the trajectories, shown in figure 5. It can be seen that we outperform the inbuilt wheel speed sensor in terms of global consistency.

TABLE III: Pose errors of our approach and the wheel speed sensors to the reference system, outdoor test drive

Pose Errors	**Ours**	Wheel Speed Sensors	Percental Enhancement
$RMSE_{\text{RPE}}$	0.105 m	0.104 m	-0.58 %
μ_{RPE}	0.057 m	0.057 m	-1.02 %
σ_{RPE}	0.088 m	0.081 m	-0.39 %
$RMSE_{\text{APE}}$	0.581 m	2.293 m	74.67 %
μ_{APE}	0.550 m	1.959 m	71.93 %
σ_{APE}	0.187 m	1.191 m	84.29 %

Additionally, we compared the Absolute Pose Error (APE) and Relative Pose Error (RPE) of both trajectories. The results are depicted in table III. While our approach keeps up with the inbuilt sensor regarding the RPE, it can be seen that it tends much less to drifts and hence has a significantly smaller APE.

VI. Discussion

In this work, we focused on implementing a robust approach to estimate velocity and yaw rate. We observed that a radar-only odometry estimation performs outstanding estimating the velocity v_x, but has weaknesses to determine the yaw rate ω. For this reason, we use the in-built IMU sensor which works complementary. The ability to measure velocity is poor since velocity is a result of integrating the measured acceleration $(a_{\text{x, IMU}})$, but the measured yaw rate has better precision compared to the radar-measured yaw rate.

By combining both sensors by an UKF, our framework is able to outperform the in-built wheel speed sensors, known as a robust method for odometry estimation, in absolute pose accuracy. Previous approaches were evaluated by a Monte-Carlo-simulation [15]. Our approach evaluates the single-shot radar odometry on real-world data for the first time. In the simulation, they achieved better results for v_x (factor 3.3), while our approach exceeded the precision for the yaw rate ω due to the UKF filtering to the factor of 9.7 and also shows significantly less drift (factor 6.6).

Assuming that the odometry estimation is combined with a localization method which is executed once every $t = 5\,\text{s}$, it will achieve errors in the same magnitude as the localization. It is hence suitable as a odometry measure for accurate localization. The average pose difference is $\mu_{\text{APE, radar-IMU}} = 0.550\,\text{m}$ and hence significantly more accurate than the wheel speed sensors, holding $\mu_{\text{APE, wheel speed}} = 1.959\,\text{m}$ in the same experiment. In addition, contrary to these sensors, our framework measures velocity correctly in cases where the vehicle gets in wheel spin or oversteering. We achieved robustness even in dynamic situations, e.g. running over a curb or performing a parking maneuver. Besides, we proved

that radar challenging environments with plenty of metal structures work satisfactory.

However, the framework shows slight effects of drifting behavior. The best way to eliminate these effects is by registering one point cloud to another [28]. If our algorithm shall be applied for loop-closure in SLAM algorithms, this step should be taken into consideration.

VII. Conclusion

We introduced a novel approach for precise odometry based on a radar belt consisting of six radar sensors and an in-built IMU sensor. The framework can be run in real-time and does not rely on GNSS methods. This makes it suitable for the use in parking applications.

Future work will combine more than the mentioned sensors. The employment of further kinematic parameters of the wheels and steering inside the framework may achieve more accurate results. Furthermore, the robustness of the approach must be analyzed more in detail. Some scenes may have hardly any radar targets and make estimation challenging since it relies on significantly less data. Besides, probabilistic approaches for motion estimation can fail if False Positive detections are not recognized.

We plan to integrate these results in an automated parking context framework to further investigate a radar-only parking solution.

References

[1] J. Levinson, J. Askeland, J. Becker, J. Dolson, D. Held, S. Kammel, J. Z. Kolter, D. Langer, O. Pink, V. Pratt, M. Sokolsky, G. Stanek, D. Stavens, A. Teichman, M. Werling, and S. Thrun, "Towards fully autonomous driving: Systems and algorithms," in *2011 IEEE Intelligent Vehicles Symposium (IV)*, Jun. 2011, pp. 163–168, iSSN: 1931-0587.

[2] M. Fazekas, P. Gáspár, and B. Németh, "Calibration and Improvement of an Odometry Model with Dynamic Wheel and Lateral Dynamics Integration," *Sensors*, vol. 21, no. 2, p. 337, Jan. 2021. [Online]. Available: https://www.mdpi.com/1424-8220/21/2/337

[3] F. Chenavier and J. Crowley, "Position estimation for a mobile robot using vision and odometry," in *Proceedings 1992 IEEE International Conference on Robotics and Automation*, May 1992, pp. 2588–2593 vol.3.

[4] T. Zhou, M. Yang, K. Jiang, H. Wong, and D. Yang, "MMW Radar-Based Technologies in Autonomous Driving: A Review," *Sensors*, vol. 20, no. 24, p. 7283, Jan. 2020. [Online]. Available: https://www.mdpi.com/1424-8220/20/24/7283

[5] E. Marti, M. A. de Miguel, F. Garcia, and J. Perez, "A Review of Sensor Technologies for Perception in Automated Driving," *IEEE Intelligent Transportation Systems Magazine*, vol. 11, no. 4, pp. 94–108, 2019.

[6] D. Nister, O. Naroditsky, and J. Bergen, "Visual odometry," in *Proceedings of the 2004 IEEE Computer Society Conference on Computer Vision and Pattern Recognition, 2004. CVPR 2004.*, vol. 1, Jun. 2004, pp. I–I, iSSN: 1063-6919.

[7] M. A. Fischler and R. C. Bolles, "Random sample consensus: a paradigm for model fitting with applications to image analysis and automated cartography," *Communications of the ACM*, vol. 24, no. 6, pp. 381–395, Jun. 1981. [Online]. Available: https://dl.acm.org/doi/10.1145/358669.358692

[8] M. He, C. Zhu, Q. Huang, B. Ren, and J. Liu, "A review of monocular visual odometry," *The Visual Computer*, vol. 36, May 2020.

[9] A. Segal, D. Hähnel, and S. Thrun, "Generalized-ICP," Jun. 2009.

[10] J. Zhang and S. Singh, "LOAM : Lidar Odometry and Mapping in real-time," *Robotics: Science and Systems Conference (RSS)*, pp. 109–111, Jan. 2014.

[11] W. Xu, Y. Cai, D. He, J. Lin, and F. Zhang, "FAST-LIO2: Fast Direct LiDAR-Inertial Odometry," *IEEE Transactions on Robotics*, vol. 38, no. 4, pp. 2053–2073, Aug. 2022.

[12] D. Barnes and I. Posner, "Under the Radar: Learning to Predict Robust Keypoints for Odometry Estimation and Metric Localisation in Radar," in *2020 IEEE International Conference on Robotics and Automation (ICRA)*, May 2020, pp. 9484–9490, iSSN: 2577-087X.

[13] Z. Hong, Y. Petillot, and S. Wang, "RadarSLAM: Radar based Large-Scale SLAM in All Weathers," in *2020 IEEE/RSJ International Conference on Intelligent Robots and Systems (IROS)*, Oct. 2020, pp. 5164–5170, iSSN: 2153-0866.

[14] D. Kellner, M. Barjenbruch, J. Klappstein, J. Dickmann, and K. Dietmayer, "Instantaneous ego-motion estimation using Doppler radar," in *16th International IEEE Conference on Intelligent Transportation Systems (ITSC 2013)*, Oct. 2013, pp. 869–874, iSSN: 2153-0017.

[15] ——, "Instantaneous ego-motion estimation using multiple Doppler radars," in *2014 IEEE International Conference on Robotics and Automation (ICRA)*, May 2014, pp. 1592–1597, iSSN: 1050-4729.

[16] C. Doer and G. F. Trommer, "An EKF Based Approach to Radar Inertial Odometry," in *2020 IEEE International Conference on Multisensor Fusion and Integration for Intelligent Systems (MFI)*, Sep. 2020, pp. 152–159.

[17] ——, "Yaw aided Radar Inertial Odometry using Manhattan World Assumptions," in *2021 28th Saint Petersburg International Conference on Integrated Navigation Systems (ICINS)*, May 2021, pp. 1–9.

[18] P. J. Rousseeuw and M. Hubert, "Anomaly detection by robust statistics," *WIREs Data Mining and Knowledge Discovery*, vol. 8, no. 2, p. e1236, 2018. [Online]. Available: https://onlinelibrary.wiley.com/doi/abs/10.1002/widm.1236

[19] R. Ghabcheloo and S. Siddiqui, "Complete Odometry Estimation of a Vehicle Using Single Automotive Radar and a Gyroscope," in *2018 26th Mediterranean Conference on Control and Automation (MED)*, Jun. 2018, pp. 855–860, iSSN: 2473-3504. [Online]. Available: https://ieeexplore.ieee.org/abstract/document/8442474

[20] H. Chen, Y. Liu, and Y. Cheng, "DRIO: Robust Radar-Inertial Odometry in Dynamic Environments," *IEEE Robotics and Automation Letters*, vol. 8, no. 9, pp. 5918–5925, Sep. 2023. [Online]. Available: https://ieeexplore.ieee.org/abstract/document/10207713

[21] A. Kramer, C. Stahoviak, A. Santamaria-Navarro, A.-a. Aghamohammadi, and C. Heckman, "Radar-Inertial Ego-Velocity Estimation for Visually Degraded Environments," in *2020 IEEE International Conference on Robotics and Automation (ICRA)*, May 2020, pp. 5739–5746, iSSN: 2577-087X. [Online]. Available: https://ieeexplore.ieee.org/abstract/document/9196666

[22] M. Goppelt, H. Bloecher, and W. Menzel, "Automotive radar–investigation of mutual interference mechanisms," *Advances in Radio Science*, vol. 8, pp. 55–60, Sep. 2010.

[23] P. H. S. Torr and A. Zisserman, "MLESAC: A New Robust Estimator with Application to Estimating Image Geometry," *Computer Vision and Image Understanding*, vol. 78, no. 1, pp. 138–156, Apr. 2000. [Online]. Available: https://www.sciencedirect.com/science/article/pii/S1077314299908329

[24] E. A. Wan and R. van der Merwe, "The Unscented Kalman Filter," in *Kalman Filtering and Neural Networks*. John Wiley & Sons, Ltd, 2001, ch. 7, pp. 221–280. [Online]. Available: https://onlinelibrary.wiley.com/doi/abs/10.1002/0471221546.ch7

[25] S. J. Julier and J. K. Uhlmann, "New extension of the kalman filter to nonlinear systems," in *Defense, Security, and Sensing*, 1997.

[26] R. Van Der Merwe and E. A. Wan, "Sigma-point kalman filters for probabilistic inference in dynamic state-space models," Ph.D. dissertation, 2004, aAI3129163.

[27] H. Hamann, J. K. Hedrick, S. Rhode, and F. Gauterin, "Tire force estimation for a passenger vehicle with the unscented kalman filter," in *2014 IEEE Intelligent Vehicles Symposium Proceedings*, 2014, pp. 814–819.

[28] H. Zhu, B. Guo, K. Zou, Y. Li, K.-V. Yuen, L. Mihaylova, and H. Leung, "A Review of Point Set Registration: From Pairwise Registration to Groupwise Registration," *Sensors*, vol. 19, no. 5, p. 1191, Jan. 2019. [Online]. Available: https://www.mdpi.com/1424-8220/19/5/1191